Molecular Mechanism of Reverse Cholesterol Transport: Reaction of Pre-β-Migrating High-Density Lipoprotein with Plasma Lecithin/Cholesterol Acyltransferase[†]

Yasushi Nakamura,[‡,§] Leila Kotite,[‡] Yonghong Gan,[#] Thomas A. Spencer,[#] Christopher J. Fielding,[‡,⊥] and Phoebe E. Fielding*[,‡,||]

Cardiovascular Research Institute, University of California, San Francisco, California 94143, Daiichi Pure Chemicals, Tokyo, Japan, Department of Medicine, University of California, San Francisco, California 94143, Department of Physiology, University of California, San Francisco, California 94143, and Department of Chemistry, Dartmouth College, Hanover, New Hampshire 03755

Received July 7, 2004; Revised Manuscript Received August 31, 2004

ABSTRACT: A 70−75 kDa high-density lipoprotein (HDL) particle with pre-β-electrophoretic migration (pre-β_1-HDL) has been identified in several studies as an early acceptor of cell-derived cholesterol. However, the further metabolism of this complex has not been determined. Here we sought to identify the mechanism by which cell-derived cholesterol was esterified and converted to mature HDL as part of reverse cholesterol transport (RCT). Human plasma selectively immunodepleted of pre-β_1-HDL was used to study factors regulating pre-β_1-HDL production. A major role for phospholipid transfer protein (PLTP) in the recycling of pre-β_1-HDL was identified. Cholesterol binding, esterification by lecithin/cholesterol acyltransferase (LCAT) and transfer by cholesteryl ester transfer protein (CETP) were measured using ^{3}H-cholesterol-labeled cell monolayers. LCAT bound to ^{3}H-free cholesterol (FC)-labeled pre-β_1-HDL generated cholesteryl esters at a rate much greater than the rest of HDL. The cholesteryl ester produced in pre-β_1-HDL in turn became the preferred substrate of CETP. Selective LCAT-mediated reactivity with pre-β_1-HDL represents a novel mechanism increasing the efficiency of RCT.

Reverse cholesterol transport (RCT)[1] of free cholesterol (FC) to plasma from peripheral cells is driven by the activity of LCAT, despite the presence within extracellular lipoproteins of significant levels of FC (*1*). Evidence of several kinds implicates small pre-β-migrating HDL particles in RCT. A 70−75 kDa lipid-poor high-density lipoprotein (HDL) particle (pre-β_1-HDL) was preferentially labeled when native plasma was incubated with mammalian cells equilibrated with ^{3}H-FC (*2*, *3*) despite rapid exchange of FC between plasma lipoproteins, particularly HDL (*4*, *5*). Isolated pre-β_1-HDL promoted efflux of cellular cholesterol (*6*). Pre-treatment of HDL with chymase, a protease selective for degrading the pre-β-migrating fraction of HDL, inhibited FC efflux (*7*). Reduction of FC efflux was also observed when native plasma was selectively depleted of pre-β_1-HDL with a monoclonal antibody (*8*). In humans, induction of pre-β_1-HDL was associated with a stimulation of RCT (*9*). In mice, an increase in pre-β_1-HDL levels led to an increase in cellular FC efflux to plasma (*10*). In contrast to the information available on this initial step of RCT, little is known about the subsequent reactions in which cell-derived FC on pre-β-HDL becomes incorporated into larger α-migrating HDL in the form of cholesteryl ester (CE). We previously reported that FC newly derived from cells was preferentially esterified by LCAT in native plasma (*2*), but neither the initial substrate nor intermediates in the formation of mature HDL were identified at that time.

Apolipoprotein A-1 (apo A-1), the presence of which defines the HDL fraction, is the only protein in most small HDLs (*2*, *3*, *11*) (including pre-β_1-HDL), as well as in a number of larger particles within the HDL fraction (*12*). Apo A-1 recycles extensively between larger lipid-rich HDLs and the lipid-poor fraction of smaller HDLs. This occurs as a result of further metabolism that includes removal of cholesteryl ester (CE) from HDL by transfer (*13*) or selective uptake (*14*) and concomitant regeneration of pre-β-HDL (*11*, *15*). PLTP also plays a key role in RCT by promoting apo A-1 recycling (*16*−*18*). It is clear that the metabolism of cell-derived FC involves multiple reaction steps beyond pre-

[†] This research was supported by the National Institutes of Health via Grants HL 57976 and HL 67294 and by Daiichi Pure Chemicals, Tokyo.

* To whom correspondence should be addressed. Mailing address: Cardiovascular Research Institute, Box 0130, University of California, San Francisco CA 94143. Tel: 415 476-3053. Fax: 415 476-2283. E-mail: pefield@itsa.ucsf.edu.

[‡] Cardiovascular Research Institute, University of California, San Francisco.

[§] Daiichi Pure Chemicals.

[#] Dartmouth College.

[⊥] Department of Physiology, University of California, San Francisco.

[||] Department of Medicine, University of California, San Francisco.

[1] Abbreviations: AEBSF, [4-(2-aminoethyl)benzenesulfonylfluoride, HCl]; CE, cholesteryl ester; CETP, cholesteryl ester transfer protein; CEFP, 4-chloro-3-ethylphenoxy-*N*-[3-(11,22-tetrafluoroethoxy)benzyl]-*N*-(3-phenoxyphenyl)-trifluoro-2-amino-2-propanol; DMS, dimethyl suberimidate·2HCl; DTNB, dithio(2-nitrobenzoic acid); FC, free cholesterol; HDL, high-density lipoprotein; LCAT, lecithin/cholesterol acyltransferase; PLTP, phospholipid transfer protein; RCT, reverse cholesterol transport.

10.1021/bi0485629 CCC: $27.50
Published on Web 10/30/2004

β_1-HDL. It is the rate of recycling of larger HDLs that seems to govern the generation of new pre-β_1-HDL and, ultimately, the rate of RCT from cells.

The development of monoclonal antibodies selective for pre-β_1-HDL (*19*, *20*) has already led to new insights into the physiological and pathological factors that determine the level of these particles in plasma. A significant increase was seen during exercise (*21*, *22*), probably reflecting a rise in the rate of recycling of apo A-1 under these conditions. Pre-β_1-HDL was increased and LCAT rates decreased in renal failure (*23*). In the present research, pre-β_1-HDL-depleted plasma generated by immunoadsorption with monoclonal antibody was used to study the formation and metabolism of this HDL fraction. The relationship between pre-β_1-HDL and plasma lipid metabolic factors LCAT, PLTP, and CETP was also studied, using selective inhibitors.

EXPERIMENTAL PROCEDURES

Reagents. Apo A-1 (>98% pure) was obtained when centrifuged normal human plasma HDL was delipidated and purified by molecular sieve chromatography (*24*). Pre-β_1-HDL-specific (Mab55201) and human LCAT monoclonal antibodies were the gift of Daiichi Pure Chemicals, Tokyo. LCAT polyclonal antibody was purchased from Novus Biologicals (Littleton, CO). Apo A-1 polyclonal antibody was from International Immunology Corporation (Murieta, CA) and apo A-2 antibody from Biodesign (Saco, ME). Horseradish peroxidase (HRP)-conjugated anti-goat IgG was from Zymed, South San Francisco, CA. 4-(2-Aminoethyl)-benzene-sulfonylfluoride (AEBSF) was from CalBiochem, San Diego, CA. 5,5′-Dithiobis(2-nitrobenzoic acid) (DTNB) was from Sigma. The 4-chloro-3-ethylphenoxy-derivative of *N*-[3-(1,1,2,2-tetrafluoroethoxy)benzyl]-*N*-(3-phenoxyphenyl)-trifluoro-2-amino-2-propanol (CEFP), a picomolar inhibitor of CETP, was synthesized as previously described (*25*). Dimethylsuberimidate·2HCl (DMS), an imidoester cross-linker of protein amines, was from Pierce, Rockford, IL.

Preparation of Pre-β_1-HDL-Deficient Plasma. Blood from normolipemic fasting volunteers was collected into ice-cooled plastic tubes containing streptokinase as anticoagulant (*26*). After centrifugation (2500 × *g*, 15 min, 0 °C), the supernatant plasma was used immediately. Ten milligrams of purified mAb 55201 IgG was covalently linked to each milliliter of CNBr-activated Sepharose 4B according to the manufacturer's instructions (Sigma, St Louis, MO). Plasma (1 mL) was mixed with 200 μL of packed slurry and incubated at 4 °C (1 h). Eluate and original plasma were assayed for their content of pre-β_1-HDL (*20*). Briefly, native or pre-β_1-HDL-depleted plasma was diluted 1/20 (v/v) into 50% sucrose solution and then 1/100 (v/v) into 1% BSA−phosphate buffered saline. Samples were added to antibody coated plates. HRP-conjugated anti-apo A-1 as second antibody was then added. Pre-β_1-HDL concentration was determined from absorbance at 492 nm with human apo A-1 as standard (*20*). Removal of 95−97% of pre-β_1-HDL immunoreactivity was obtained.

Nondenaturing Gradient Polyacylamide Gel Electrophoresis (*PAGE*). Single dimension PAGE was carried out with precast 10−20% w/v polyacrylamide gradient gels (Biorad, Hercules, CA). Plasma samples were diluted (2-fold) in 31% sucrose, 0.06% EDTA, 0.01% bromophenol blue to stabilize pre-β_1-HDL levels (*20*), then electrophoresed, together with globular protein standards of known molecular weight (HMW Native, Amersham Biosciences, Piscataway, NJ). In some studies, ovalbumin (Sigma, MW 41 kDa) was included as an additional marker. Fractionation was carried out in 90 mM Tris, 80 mM boric acid, 3 mM EDTA (pH 8.3) at 75 V (20 h, 4 °C). In some experiments, electrophoresis of the same plasma sample was carried out over a range of times (8−32 h) to identify any effects on the apparent molecular weight (MW_{app}) of HDL fractions relative to protein standards. After electrotransfer to nitrocellulose membranes (0.2 μM pore), blocking was carried out using 5% w/v skim milk in 20 mM Tris-HCl, 0.15 M NaCl, pH 7.4 containing 0.1% Tween 20. Membranes were incubated with the primary antibody indicated, then with second antibody conjugated to horseradish peroxidase, and finally with Supersignal chemiluminescent substrate (Pierce, Rockford, IL)(*27*). Blots were visualized with Hyperfilm ECL X-ray film (Amersham Biosciences). The relative concentration of antigen in different HDL species was determined by computerized scanning densitometry.

For two-dimensional nondenaturing electrophoresis, HDL in plasma was first fractionated in 0.8% w/v agarose in 0.025 M barbital buffer (pH 8.6) (*2*). A 2−3 mm strip from this gel was laid lengthwise on a precast 1 mm 10−20% v/v polyacrylamide gradient gel. Second dimensional electrophoresis, electrotransfer and immunoblotting were then carried out as above.

Cross-Linking Two-Dimensional Electrophoresis. To assess the number of apo A-1 molecules in individual HDL species, native plasma, along with molecular weight marker proteins, was first fractionated by nondenaturing electrophoresis in 10−20% polyacrylamide gradients. Two to three millimeter wide vertical strips from plasma lanes of the gel were rinsed with distilled water, incubated (20 min, 20 °C) with two changes of 0.1 M triethanolamine, pH 9.7, and then with DMS (4 mg mL^{-1}) in the same buffer (2 h, 20 °C)-(*28*). Control gel strips were incubated in the presence of triethanolamine without cross-linker.

Gel strips containing cross-linked proteins were rinsed with distilled water, incubated with 0.125 M Tris-HCl, 2% SDS, pH 6.8 (60 °C, 2 h) and then laid over 1.5 mm thick 10% polyacrylamide gels. Electrophoresis in the second dimension was carried out in 0.19 M glycine, 0.025 M Tris-HCl, 0.1% SDS, pH 8.9. Following electrotransfer of the gel to nitrocellulose membranes, immunoblotting was carried out with apo A-1 antibody. The presence of monomeric and cross-linked apo A-1 bands in HDL fractions of native plasma was determined from their migration rate vs protein standards.

Cell Culture. Normal human primary skin fibroblasts grown in 3.5 cm dishes to near confluence were equilibrated (48 h, 37 °C) in 10% v/v fetal bovine serum (FBS)−Dulbecco's modified Eagle's medium (DME) containing 1,2-[^{3}H]-cholesterol (51 Ci/mmol, Perkin-Elmer/NEN, Boston, MA; 50 μCi/dish). After washing (×2) in PBS, incubation with unlabeled native plasma was carried out at 37 °C for 0.25−120 min. Samples of medium were then cooled in ice water and fractionated by nondenaturing gradient gel electrophoresis. After electrotransfer, HDL species identified by apo A-1 or LCAT antibody blots were cut out and extracted into 1/1 v/v chloroform/methanol. Thin-layer chromatography

Table 1: Rates of Cholesterol and Phospholipid Metabolism and the Effects of Inhibitors and Activators[a]

condition	LCAT	PLTP	CETP
control	52.8 ± 11.9	70.0 ± 50.8	16.1 ± 5.3
+ DTNB (1.4 mM)	9.0 ± 6.4	26.1 ± 19.3	15.8 ± 7.3
+ AEBSF (10 mM)	0.0[b]	252.3 ± 102.6	*c*
+ CEFP	43.9 ± 17.8	82.6 ± 29.0	0.0[b]

[a] Plasma FC was 1.24 ± 0.07 mM. Rates are expressed as nmol mL^{-1} of plasma h^{-1}. Values are means ± 1 SD (n = 3−5). [b] Undetectable. [c] Not determined, since the assay of HDL CE using cholesterol esterase is blocked by serine protease inhibitors (*53*).

of the chloroform phase with unlabeled FC and CE as standards was carried out using silica gel on plastic sheets developed in hexane/diethyl ether/acetic acid 83/16/1 v/v. FC and CE were identified with iodine vapor. ^{3}H-radioactivity in these bands was determined by liquid scintillation spectrometry.

Assays of LCAT and PLTP Activities. LCAT activity in plasma was assayed as the rate of decrease of FC mass at 37 °C (*29*). CETP activity was measured as the rate of decrease in HDL CE under the same conditions (*30*). PLTP activity was expressed as the rate of transfer of PL from very low-density lipoproteins (VLDL) and low-density lipoproteins (LDL) to HDL at 37 °C, measured in HDL following precipitation of VLDL and LDL with Mg^{2+}/dextran sulfate (*30*). HDL phospholipid was determined after phospholipase digestion, using choline oxidase (Wako Chemicals, Richmond, VA).

In some incubations, final concentrations of 10 mM AEBSF, 1.4 mM DTNB, or 10 μM CEFP were added to plasma prior to incubation. In other assays, plasma was preincubated (2 h, 0 °C) with mAb55201−Protein G−agarose. After centrifugation to remove pre-β_1-HDL bound to the agarose beads, assays of HDL fractions were carried out in the presence or absence of cultured fibroblast monolayers.

RESULTS

Lipid Metabolic Activities in Human Plasma. LCAT, CETP, and PLTP activities in native or pre-β_1-HDL-depleted (mAb55201-adsorbed) plasma were determined in the presence or absence of inhibitors (Table 1). LCAT was strongly inhibited by DTNB, a sulfhydryl inhibitor (*31*), probably via the free cysteine group (C_{184}) adjacent to active site serine residue S_{181} (*32*, *33*). LCAT was also completely inhibited by AEBSF, a serine protease inhibitor (*34*, *35*). DTNB inhibited PLTP activity (−66%) possibly reflecting the presence of a cysteine residue (C_{21}) adjacent to the essential arginine (R_{25}) within the PLTP N-terminal HDL binding pocket (*36*, *37*). In contrast, AEBSF increased PLTP activity 4-fold. Plasma CETP activity was unmodified by DTNB but was completely inhibited in the presence of CEFP. These selective inhibitors were used to differentiate the roles of PLTP, LCAT, and CETP in HDL speciation.

Distribution of apo A-1 in HDL. Following nondenaturing electrophoresis of plasma, the MW_{app} of component HDL fractions was determined from their migration rates relative to globular protein standards (Figure 1). Their concentration under different conditions was determined with apo A-1 polyclonal antibody using scanning densitometry. The densitometric results described below represent means ± 1 SD from three to four independent experiments. There was no

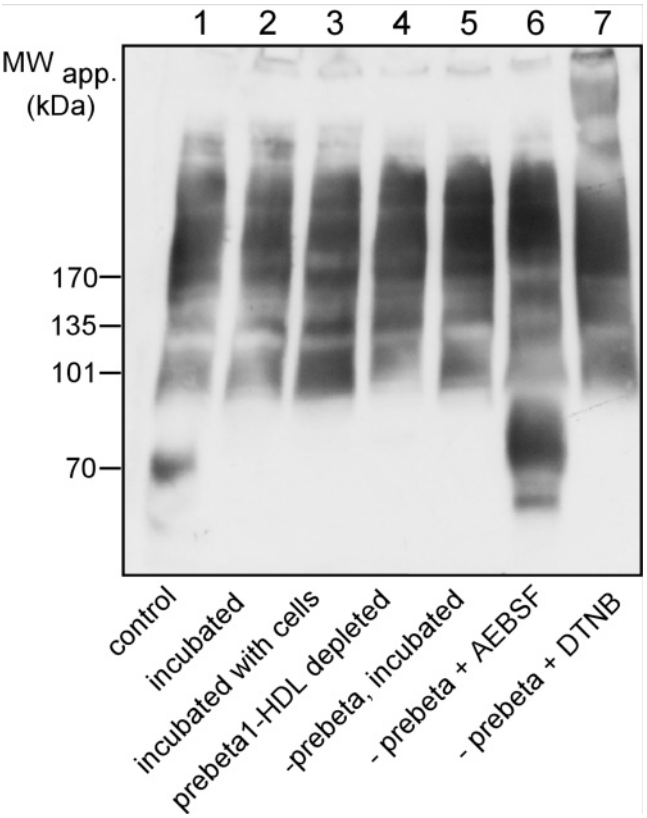

FIGURE 1: Human plasma HDL fractions following one-dimensional nondenaturing electrophoresis, identified with apo A-1 antibody: lane 1, native human plasma; lane 2, after incubation (2 h, 37 °C) in the absence of cells; lane 3, the same in the presence of a human fibroblast monolayer; lane 4, nonincubated plasma after absorption with mAb 55201; lane 5, the same after incubation (2 h, 37 °C); lane 6, the same after incubation with AEBSF (10 mM); lane 7, the same after incubation with DTNB (1.4 mM). Molecular weight markers were thyroglobulin (MW 669 000); ferritin (MW 440 000); catalase (MW 232 000); lactate dehydrogenase (MW 140 000), and albumin (MW 66 000).

significant difference in estimated size after electrophoresis over 8−32 h for any HDL fraction (data not shown). Electrophoresis time (normally 18−22 h) was chosen for optimal separation in the 50−200 kDa size range.

Apo A-1 in the <200 kDa size range was present not as a continuum but in a series of bands. Some HDL, representing ~3% of total apo A-1, was present as a rapidly migrating subfraction (Figure 1, lane 1)(*2*, *3*) the MW_{app} of which was 70 ± 2 kDa. A minor fraction of 54 ± 4 kDa was sometimes seen. Other apo A-1 bands of MW_{app} 101 ± 4, 135 ± 3, and 170 ± 4 kDa, were also identified. The rest of the apo A-1 antigen was present in zones of higher MW_{app} (>200 kDa). As previously reported (*2*), apo A-2 was absent from the smaller HDL species (data not shown). Comparison of one- and two-dimensional electrophoresis patterns from the same plasma samples showed that the 70 kDa HDL had equivalent pre-β-electrophoretic migration, while other fractions had α-mobility (data not shown), confirming the identity of the 70 kDa HDL fraction as pre-β_1-HDL (*2*).

When native plasma was incubated at 37 °C, apo A-1 in pre-β_1-HDL was significantly (−90% ± 4%) decreased (Figure 1, lane 2) as previously described (*26*). The distribution of other bands was not substantially changed. After incubation in the presence of a cultured cell (fibroblast)

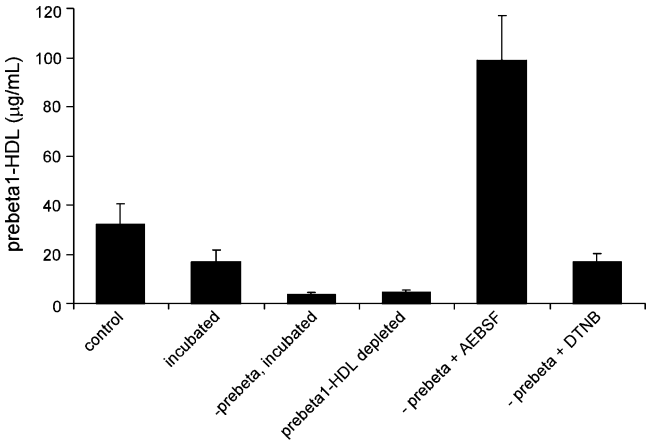

FIGURE 2: Immunoassay of pre-β-HDL with Mab 55201. Values are means ± one SD of 10 separate experiments. Conditions for fractionation and incubation are the same as those described in the legend to Figure 1.

monolayer, apo A-1 in both 101 and 135 kDa bands increased (1.82 ± 0.10)-fold (Figure 1, lane 3). Immunoabsorption of plasma with pre-β_1-HDL specific antibody (mAb 55201) at 0 °C led to an almost complete loss of apo A-1 in the 54 and 70 kDa bands (Figure 1, lane 4). There was a slight increase in the 135 kDa band. Incubation of immunoadsorbed plasma (2 h, 37 °C) led to an increase ((1.70 ± 0.10)-fold) in 101 kDa HDL, as well as a smaller increase (+30%) in larger (135 and 170 kDa) HDLs. The pre-β_1-migrating HDL 70 kDa fraction was not significantly regenerated under these conditions (Figure 1, lane 5).

Incubation of immunoadsorbed plasma in the presence of either AEBSF (which blocked LCAT but activated PLTP) or DTNB (which inhibited both LCAT and PLTP) gave different results. In the presence of AEBSF, there was a substantial increase in pre-β_1-HDL to a level that exceeded by (4.5 ± 1.0)-fold the concentration in native plasma (Figure 1, lane 6). There was a slight increase (+10 ± 2 kDa) in the MW_{app} of this pre-β_1-HDL compared to control, suggesting that elevated PLTP activity in the presence of AEBSF might have increased its PL content. The 101 and 135 kDa HDL fractions were decreased (−76% and − 80%, respectively) and replaced by novel species (MW_{apps} 115 and 145 kDa). Incubation with DTNB (2 h, 37 °C) did not increase apo A-1 in the 70 kDa band or modify the distribution of apo A-1 antigen in other HDL fractions, apart from the appearance of small amounts of apo A-1 in high molecular weight species (Figure 1, lane 7). As LCAT was inhibited by both AEBSF and DTNB, the changes seen in lane 6 (compared to lane 7) are likely to mainly reflect increased PLTP activity.

Levels of pre-β_1-HDL in plasma under the conditions just described were also determined by solid-phase immunoassay (Figure 2). Incubation of native plasma (2 h, 37 °C) led to a decrease (−50% ± 8%) in pre-β_1-HDL levels. This change was less than that assayed following electrophoresis. The difference may reflect the stability of pre-β_1-HDL in sucrose (*20*). Adsorption of native plasma with mAb 55201 led to removal of >95% of immunoreactivity, consistent with the electrophoresis data. Pre-β_1-HDL levels in immunodepleted native plasma hardly increased during incubation (2 h, 37 °C), also consistent with the data in Figure 1. Incubation of pre-β_1-HDL-depleted plasma with AEBSF was associated with a significant increase in pre-β_1-HDL to levels that were (2.8 ± 0.5)-fold those in native plasma, indicating reactivity of mAb55201 with both 70 and 80 kDa pre-β_1-HDL particles. Incubation of immunodepleted plasma in the presence of DTNB increased pre-β_1-HDL levels to 25% of those seen with AEBSF.

Taken together, the data in Figures 1 and 2 indicate PLTP to be a major factor determining plasma pre-β_1-HDL levels. AEBSF treatment was also associated with the appearance of novel small HDL fractions, possibly representing intermediates in PLTP-dependent generation of pre-β_1-HDL from larger particles.

Cross-Linking Two-Dimensional Electrophoresis. Native HDLs of different MW_{app} seen in this study could represent products of stepwise addition of apo A-1 (28 kDa). Alternatively, they might reflect the transfer of lipids. The presence of cross-linked apo A-1 multimers in HDL species was investigated using two-dimensional electrophoresis. In the absence of cross-linker, only apo A-1 monomer (MW 28 kDa) was present (data not shown). After cross-linking, in the absence and more strikingly in the presence of AEBSF, only monomeric apo A-1 was detected in pre-β_1-HDL (Figure 3). In the absence of AEBSF, 101 kDa HDL included some dimer, while the 135 kDa fraction of HDL contained substantial amounts of dimeric apo A-1 (58 kDa). Both species also contained apo A-1 monomer (Figure 3, left panel). In the absence of AEBSF, several unassigned bands with MW_{app} between 28 and 57 kDa were also present. The 170 kDa and larger HDL fractions contained cross-linked species of higher molecular weight. Increased levels of pre-β_1-HDL were seen when AEBSF was present (Figure 3, right panel) consistent with the data in Figures 1 and 2. The 110 kDa HDL under these conditions appeared to also contain mostly monomer, the higher molecular weight species containing dimer and larger bands. These data suggest that interconversion of pre-β_1-HDL and 110 kDa HDL (+AEBSF) or 101 kDa HDL (−AEBSF) mainly reflect the addition or subtraction of lipids. The data also indicate that either pre-β_1-HDL contains a single apo A-1 or, more likely, they are resistant to cross-linking under our conditions.

LCAT in Native Plasma. LCAT is recognized to be the major determinant of HDL speciation in plasma (*11*). It also plays an important role in facilitating RCT (*2*). Therefore, the effect of the perturbations described above on the distribution of LCAT antigen among HDL subfractions in plasma was determined. LCAT binding to HDL increases MW_{app} by 59 kDa (Table 2) (*38*). As previously reported (*39*) LCAT is distributed among several HDL fractions in native plasma (Figure 4, lane 1). In the present studies, >80% of total antigen, by scanning densitometry, migrated with MW_{app} >230 kDa. This presumably reflects complex formation of LCAT with HDL of >170 kDa. Binding of more than one LCAT per HDL particle is not excluded but is unlikely in view of the high concentration in plasma of apo A-1 (~1400 μg mL^{-1}, *19*) compared to that of LCAT (7−10 μg mL^{-1}, *40*), a 300-fold excess. The second major LCAT fraction in native plasma had a MW_{app} of 135 ± 10 kDa corresponding to a complex between LCAT and an HDL fraction of ~75 kDa. A faint band of MW_{app} 165 kDa was also seen (corresponding to an HDL of ~105 kDa). No LCAT migrated near albumin (MW 67 kDa) indicating an absence of detectable free LCAT in native plasma. As was

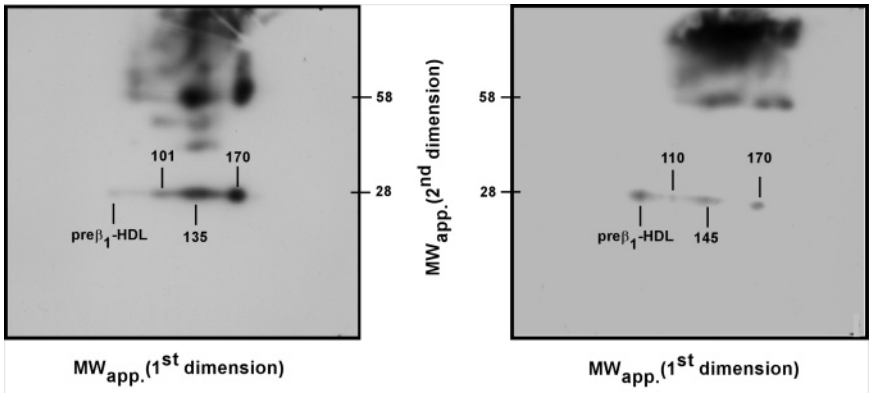

FIGURE 3: Cross-linking two-dimensional electrophoresis of HDL in native human plasma. First dimension nondenaturing gradient electrophoresis (left to right) was followed by cross-linking within the gel using DMS. Second-dimensional SDS electrophoresis was carried out to separate apo A-1 monomers and oligomers on the basis of their molecular weight. Following electrotransfer, apo A-1 was identified by Western blotting with apo A-1 polyclonal antibody. The left panel shows fractionation of native plasma. The right panel shows fractionation of plasma with AEBSF. Horizontal scale is the MW_{app} of native HDL species. Vertical scale is the MWs of apo A-1 species after cross-linking. These were determined with nondenaturing and SDS gel protein standards, respectively.

Table 2: MW_{app} of HDL Subfractions[a]

assayed with A-1 antibody	assayed with LCAT antibody	corrected values from LCAT antibody assay
70 ± 2[b]	*c*	
101 ± 4	*c*	
135 ± 3	135 ± 10	76 ± 10[d]
170 ± 4	165 ± 5	106 ± 5[e]
195 ± 6	195 ± 8	136 ± 8[f]

[a] The MW_{app} of HDL fractions in terms of apo A-1 antibody (column A) was determined as shown in Figure 1. The MW_{app} of the same HDL fractions assayed with anti-LCAT antibody (column B) was determined as shown in Figure 4. HDL MW_{apps} assayed with LCAT antibody were corrected for the presence of LCAT by subtracting 59 kDa (last column) (*38*). [b] Pre-β_1-HDL. [c] LCAT antigen was undetectable in these fractions. [d] Not significantly different from pre-β-HDL. [e] Not significantly different from the 101 kDa. [f] Not significantly different from135 kDa.

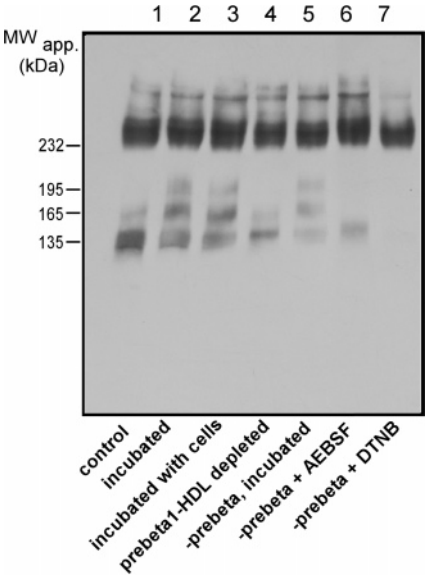

FIGURE 4: Human plasma fractions following one-dimensional nondenaturing electrophoresis identified with LCAT antibody. Conditions for fractionation and incubation are the same as those described in the legend to Figure 1.

the case for apo A-1, in small HDLs it is apparent that LCAT antigen bound to HDL was present in the form of a few discrete bands.

Incubation of plasma (2 h, 37 °C) led to significant changes in LCAT distribution (Figure 4, lane 2). While LCAT antigen in the 135 kDa fraction decreased ($-48\% \pm 10\%$), that in the 165 kDa and especially in a new ~195 kDa fraction (corresponding to an HDL of about 135 kDa) both increased ($+432\% \pm 40\%$). Total LCAT antigen in the combined 135, 165, and 195 kDa fractions was unchanged. This result suggested that the effect of incubation was limited to LCAT bound to smaller HDL and that these might represent the major metabolically active fraction of the enzyme in plasma. The presence of a cell monolayer did not modify the distribution of LCAT antigen (Figure 4, lane 3). Removal of pre-β_1-HDL from native plasma with mAb 55201 decreased LCAT antigen in the 135 and 165 kDa bands (-30% and -60%, respectively)(Figure 4, lane 4). Following incubation (2 h, 37 °C) of pre-β_1-HDL-depleted plasma, 165 and 195 kDa LCAT bands were regenerated (Figure 4, lane 5). The increase on incubation was inhibited ($-90\% \pm 4\%$) by either AEBSF or DTNB (Figure 4, lanes 6 and 7). These data support a model in which LCAT binds directly to pre-β_1-HDL.

To study further the possible relationship between pre-β_1-HDL and the 135 kDa LCAT-containing fraction, increasing volumes of monoclonal LCAT antibody were added to native plasma. A progressive increase of apo A-1 in pre-β_1-HDL was seen, primarily in the 70 kDa fraction, reaching a maximum of 4.5-fold. Simultaneously there was a loss of apo A-1 from the 101 kDa fraction ($-70\% \pm 10\%$) and from 135 kDa HDL ($-75\% \pm 10\%$)(Figure 5). These data indicate that LCAT activity was a major factor determining its own distribution between HDL species. PLTP in the absence of LCAT activity had little or no effect on LCAT distribution. The relationship demonstrated between the 135 kDa LCAT fraction and pre-β_1-HDL is also consistent with the former representing a complex between pre-β_1-HDL and LCAT.

Metabolism of Cell-Derived FC in HDL Fractions. Fibroblasts equilibrated with ^{3}H-FC were used to determine whether the distribution of LCAT antigen among HDL species reflected enzyme activity and whether formation of ^{3}H-CE was causative for the redistribution of antigen during incubation at 37 °C. ^{3}H-FC-labeled cell monolayers were incubated with native human plasma. At intervals, samples of medium were collected and processed by nondenaturing

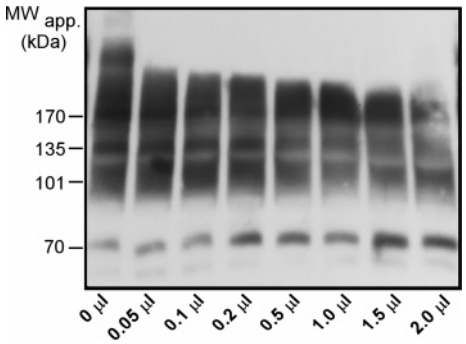

FIGURE 5: The effect of increasing levels of LCAT mAb on the distribution of apo A-1 in native plasma. Incubation (2 h, 37 °C) was followed by rapid cooling and nondenaturing gel electrophoresis as shown in Figure 1.

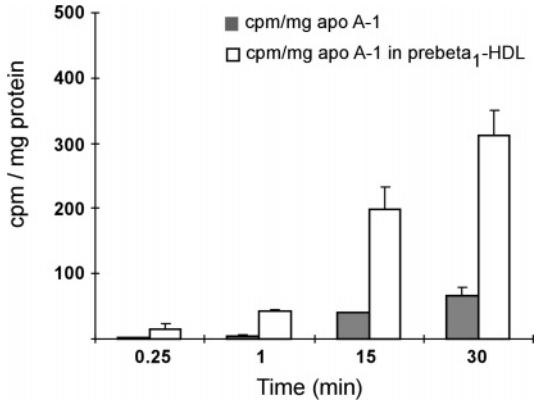

FIGURE 6: Plasma ^{3}H-FC in pre-β_1-HDL and total HDL in the presence of human fibroblasts. Label is expressed in terms of apo A-1 in the pre-β_1-HDL fraction after nondenaturing electrophoresis and of total plasma apo A-1. These were determined by immunoassay with mAb55201 and with polyclonal apo A-1 antibodies, respectively.

gel electrophoresis, electrotransfer, and thin-layer chromatography of the extracted bands. When the data were normalized to the mass of apo A-1 in pre-β_1- and total HDL, FC-specific activity was initially (0.25 min) 7−8-fold greater in the pre-β_1-HDL fraction. Averaged over 0.25−30 min, it was (5.0 ± 0.7)-fold greater (Figure 6). No label was detected in the 54 kDa HDL fraction when it was present.

At 0.25 min no ^{3}H-CE was recovered in any fraction, indicating FC to be the only form of cellular sterol transferred from the fibroblast monolayer to plasma. At 15 min of incubation, a significant level of ^{3}H-CE was recovered in the smaller HDL fractions. The highest (39% ± 12% of total plasma ^{3}H-CE) was recovered in the 135 kDa region (Figure 7, panel A) even though by densitometry this contained <5% of total apo A-1 antigen. As a result, this fraction was enriched ~8-fold in ^{3}H-CE compared to ^{3}H-CE label in total HDL. ^{3}H-CE was also found in the 170 and 200 kDa fractions, following kinetics suggestive of a precursor−product relationship between 135 kDa and larger LCAT-containing HDLs. A small amount of ^{3}H-CE was measured in the 101 kDa band the contribution of which peaked at 30 min incubation. This may represent label from 170 kDa particles from which LCAT has dissociated, since no LCAT antigen was observed in association with this molecular weight. Though large (>230 kDa) HDL contained >80% of LCAT antigen determined by immunoblot (Figure 4), these particles contained <15% of ^{3}H-CE at all time points

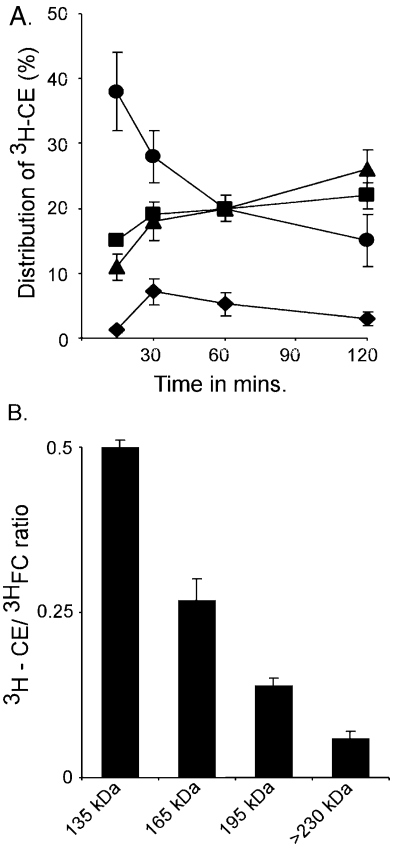

FIGURE 7: Panel A shows the distribution of ^{3}H-CE between HDL LCAT-containing fractions detected with LCAT antibody as a function of time following incubation with ^{3}H-FC labeled fibroblast monolayers: (◆) 101 kDa fraction; (●) 135 kDa LCAT fraction; (■) 165 kDa LCAT fraction; (▲) 195 kDa LCAT fraction. Values shown are means ± one SD (n = 4). ^{3}H-CE in MW_{app} 101 kDa HDL (◆) probably represents label in particles from which LCAT has dissociated (see text). Panel B shows the ^{3}H-CE/^{3}H-FC ratio in HDL fractions following incubation of native plasma with ^{3}H-FC labeled cells. The data shown represents the means ± one SD of four experiments assayed after incubation for 2 h, 37 °C.

after incubation with cells, consistent with the hypothesis that LCAT bound to small HDL is metabolically the most active.

Further information on relative rates of LCAT activity was obtained by determining the ratio of ^{3}H-CE and ^{3}H-FC in each HDL fraction. After 120 min, in large (>230 kDa) HDLs, this ratio was 0.06, similar to the rate of LCAT activity in whole plasma, where 0.08 (106/1240 nmol) of total FC was esterified over the same time period (Table 1). In the 135 kDa fraction, which may represent a complex between LCAT and pre-β_1-HDL, this ratio was 0.50 or 8-fold higher. In the 165 and 195 kDa fractions, intermediate ratios were found (Figure 7, panel B). These data are consistent with the concept that the 135 kDa fraction including LCAT generates much of the ^{3}H-CE later seen in other fractions.

The relatively low level of ^{3}H-CE in large HDL (the major apo A-1 containing fraction) was unexpected. Two factors could explain this finding. Label originating here would be underestimated if large HDLs were the preferred substrate for CETP. Alternatively, CETP might be mainly active in the transfer from small HDL of ^{3}H-CE that had recently originated as cellular ^{3}H-FC. To distinguish these alternatives, the effect of CETP inhibition on the level and distribution of ^{3}H-CE among HDL fractions was determined. CETP

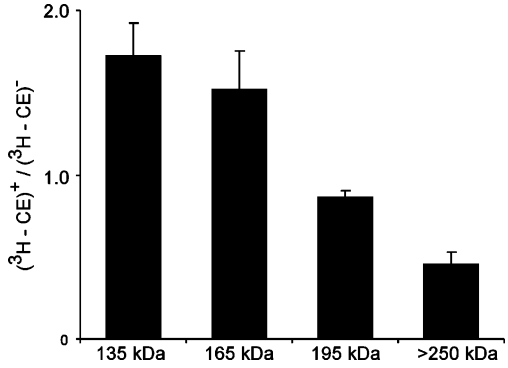

FIGURE 8: Effects of CEFP on the recovery and distribution of ^{3}H-CE generated in the presence of ^{3}H-FC labeled human fibroblasts. The vertical axis is a ratio of CE formed in the presence compared to the absence of CEFP. Incubation conditions were as described in the legend to Figure 7. The data are means ± one SD of four experiments. A ratio >1 indicates that HDL fraction to be a net donor of ^{3}H-CE in the presence of CETP activity. A ratio <1 indicates that HDL fraction to be a net acceptor of ^{3}H-CE under the same conditions.

activity in native plasma (16.1 ± 5.3 nmol mL^{-1} of plasma h^{-1})(Table 1) was 0.3 ± 0.04 relative to the molar rate of LCAT activity, indicating two-thirds of LCAT-derived cholesteryl esters in plasma are retained in HDL. In plasma that had been incubated with ^{3}H-FC labeled cells, there was a significant increase (+30% ± 3%) in total ^{3}H-CE in the 135, 165, and 195 kDa fractions when CEFP was present (Figure 8). The greatest effect was seen in the smallest of these HDLs, suggesting this to be the source of most of the ^{3}H-CE normally transferred from small HDL to other lipoproteins (VLDL, LDL). There was a significant reduction in the level of ^{3}H-CE, already low, in larger HDLs in the presence of CEFP indicating that part of ^{3}H-CE present in the largest HDLs in the absence of inhibitor had been transferred there from smaller, more active particles.

The data obtained with ^{3}H-FC-labeled cells make several major points. The proportion of cell-derived FC relative to apo A-1 was greatest in pre-β_1-HDL, confirming earlier observations (*2*, *3*). Most CE formed from cell FC was found in smaller HDL particles, even though the greatest part of LCAT antigen was in large HDL. On incubation of plasma, the distribution of labeled CE increased to HDL particles of larger molecular weight, as did the distribution of LCAT antigen. This indicated that most LCAT remained associated with the growing substrate particles during the period of incubation. As a result, ^{3}H-CE in a 135 ± 10 kDa particle identified with LCAT antibody reflected the reaction of LCAT (59 kDa) with FC in a 76 ± 10 kDa HDL (Table 2). Comparable conclusions apply to larger ^{3}H-CE-labeled HDL fractions.

The proportion of label esterified was much greater than that expected if cell FC had equilibrated with plasma lipoproteins. This means that there was a preferential esterification of cell-derived FC by LCAT. Finally, the metabolically active HDL species most enriched with ^{3}H-CE were also the best substrates for CETP.

DISCUSSION

LCAT plays a key role in a cycle during which its product, CE, is transferred out of larger HDLs while pre-β_1-HDL is regenerated (*11*) allowing reutilization of these particles for RCT. Recent data suggest HDL may bind directly both to FC-rich microdomains of the cell surface as part of a raft/caveola-dependent FC efflux pathway (*41*) and to sites of ABCA1-mediated FC efflux (*42*). The potential of these pathways to drive RCT would be quickly dissipated if diffusion of FC back to the cell were not inhibited. The present study identifies FC esterification mediated by preferential binding of LCAT to pre-β_1-HDL as a mechanism to more efficiently sequester cell-derived FC as CE in extracellular HDL.

Roles of PLTP and Pre-β_1-HDL. AEBSF, which binds covalently to active site serine residues, stimulated PLTP activity both in terms of PL transfer from VLDL and LDL to HDL and in the formation of pre-β_1-HDL. Proteases in plasma such as chymase can degrade and inactivate PLTP and also cleave apo A-1 in the pre-β_1-fraction to a 14 kDa product (*7*, *43*). It seems unlikely that these factors explain the changes in pre-β_1-HDL concentration and properties associated with increased PLTP activity. HDL completely prevented the degradation of PLTP (*7*), and no degradation product was seen in either the presence or the absence of AEBSF (Figure 3). However, the increase in PLTP activity induced by AEBSF, together with the inhibition of LCAT, has provided considerable insight into the HDL cycle. One major activity of PLTP is evidently to generate pre-β_1-HDL, consistent with earlier reports (*44*, *45*). As the 145 and 115 kDa fractions accumulate only in the presence of AEBSF, when further metabolism of pre-β_1-HDL is inhibited, it appears likely that these represent intermediates in the formation of pre-β_1-HDL from larger HDL precursors by loss of apo A-1 and phospholipids. Similarly, on the basis of cross-linking electrophoresis, stepwise increases in HDL size seen in response to LCAT activity appear to reflect the addition of lipids and apo A-1 subunits to pre-β_1-HDL. Pre-β_1-HDL was preferentially labeled with cell-derived ^{3}H-FC, consistent with previous data (*2*, *3*) and the role of this particle as a major primary initiator of RCT (*11*). The same particle thus appears to be both the main end-product of PLTP activity and also the major initial substrate for RCT and LCAT by the recycling pathway (Figure 9). Small amounts of a 54 kDa pre-β-HDL were seen in some experiments and may represent a distinct (pre-β_0-) HDL fraction otherwise identified only in diabetic and diluted normal plasma (*46*, *47*). In the present studies, 54 kDa HDL did not bind cell-derived FC; as a result it is probably not directly involved in RCT. Synthetic poorly lipidated HDLs containing a single apo A-1 have been described (*48*), but these had less lipid than pre-β_1-HDL particles in plasma (*2*). A recent study reports that similar particles had α-electrophoretic mobility (*49*). Further research on the structure of these particles is needed.

Role of LCAT. Most LCAT antigen was associated with large HDL, but most LCAT activity, at least with cell-derived ^{3}H-FC, was mediated by enzyme recovered with smaller HDL. This finding has major implications for the mechanism of RCT. If pre-β_1-HDL, enriched in cell-derived FC, were also an optimal substrate for LCAT, the efficiency of RCT would be significantly increased. The MW_{app} of the smallest HDL to contain LCAT was 135 ± 10 kDa, consistent, within experimental error, with a complex of pre-β_1-HDL (70 ± 2 kDa) and LCAT (Table 2). LCAT bound to an HDL particle increases its MW_{app} by 59 kDa (*38*). The 135 kDa fraction

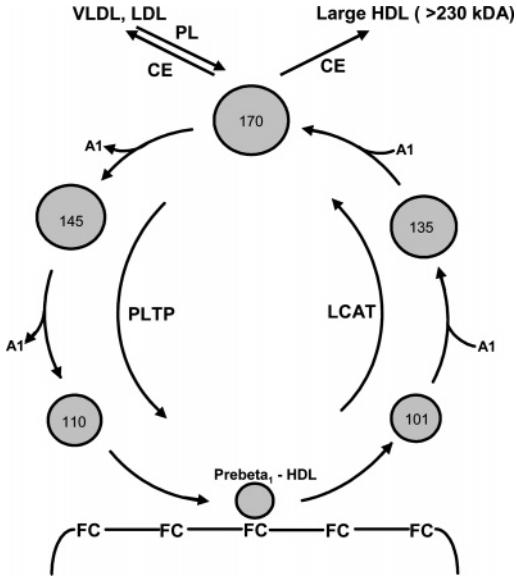

FIGURE 9: A model suggesting relationships among HDL fractions in human plasma and the roles of LCAT and PLTP. To enable comparison to be made between HDL species in the cycle, MW_{apps} are given in terms of apo A-1 and lipid content only.

showed the greatest enrichment with ^{3}H-CE, relative both to ^{3}H-FC and to ^{3}H-CE. The time course of ^{3}H-CE distribution between HDL fractions was consistent with a precursor-product relationship. When LCAT was removed from native plasma with a monoclonal antibody, the level of pre-β_1-HDL increased. Removal of pre-β_1-HDL with mAb55201 depleted LCAT antigen within the 135 kDa fraction. This may indicate reactivity of this antibody with pre-β_1-HDL even when it is part of a complex with LCAT. Alternatively, removal of pre-β_1-HDL may dissociate a 135 kDa complex, redistributing LCAT to other HDL fractions. Titration of plasma with LCAT antibody was associated with the appearance of increased levels of pre-β_1-HDL. Finally, as CE formation continued, discrete fractions containing LCAT antigen and with increasing MW_{app} were generated. Like the 135 kDa LCAT complex, these contained ^{3}H-CE. Taken together, these data provide strong evidence for complex formation between LCAT and pre-β_1-HDL. They also emphasize the important role of a minor population of relatively small HDL in RCT (Figure 9). The SR−BI pathway can facilitate the uptake of FC as well as CE into cells (*50*). In principle, cell-derived FC bound to pre-β_1-HDL might be directly internalized by this route, bypassing the LCAT reaction. However, it has been shown that this HDL fraction binds only poorly to SR−BI (*51*).

Role of CETP. The HDL cycle is driven by incorporation of substrate (FC, in particular cell-derived FC) and by loss of product (CE). In vivo, two pathways can remove CE from HDL: CE transfer to other lipoproteins (VLDL, LDL, other HDL) mediated by CETP (*13*) and selective uptake of HDL-CE mediated by SR−BI (*14*). Cultured fibroblasts expressed only very low levels of SR−BI (*52*). As a result, the role of CETP in processing cell-derived FC could be assessed by comparing the distribution of ^{3}H-CE in the presence and absence of its inhibitor (CEFP). Blocking CETP activity significantly increased the level of ^{3}H-CE retained in small HDL, specifically the 135 and 170 kDa LCAT−HDL complexes. Under the same conditions, ^{3}H-CE decreased in large HDL. These data show that as in the case of LCAT, CETP activity was primarily directed toward small, metabolically active HDL ultimately derived from pre-β_1-HDL. Further research will be needed to determine whether CE in these particles is selectively cleared by the SR−BI pathway. If this is the case, CETP inhibitors could have even greater effects on plasma HDL metabolism than would appear from changes in HDL CE levels.

Efficiency of RCT. LCAT activity in whole plasma (55 nmol h^{-1} mL^{-1}) esterified 27.5/1226 nmol (that is, 1.9%) of FC to CE over 30 min at 37 °C. If cell-derived ^{3}H-FC completely equilibrated with plasma lipoproteins prior to esterification, this proportion of total label (1.9%) would be esterified. In contrast, over the same time period, 30% of cell-derived ^{3}H-FC was esterified and recovered in the 135 kDa LCAT fraction. If labeled CE in the 165 and 195 kDa LCAT fractions originated from the 135 kDa fraction, as appears from the present studies, the total of cell-derived FC esterified on pre-β_1-HDL and its products was 70% of total ^{3}H-CE formed. This fraction was only slightly reduced over more extended (120 min) incubation. These values suggest that direct esterification of cell-derived FC on pre-β_1-HDL greatly increases the efficiency of RCT.

In summary, changes in the distribution of small HDL species induced by immunoabsorption, inhibitors or incubation gave information on early steps of RCT between the cell surface and HDL and provided a possible explanation for the effectiveness of these species in regulating peripheral FC accumulation.

ACKNOWLEDGMENT

The excellent technical support of Lourdes Escoto is acknowledged.

REFERENCES

1. Fielding, C. J., and Fielding, P. E. (1981) Evidence for a lipoprotein carrier in human plasma catalyzing sterol efflux from cultured fibroblasts and its relationship to lecithin: cholesterol acyltransferase, *Proc. Natl. Acad. Sci. U.S.A. 78*, 3911−3914.
2. Castro, G. R., and Fielding, C. J. (1988) Early incorporation of cell-derived cholesterol into pre-β-migrating high-density lipoprotein, *Biochemistry 27*, 25−29.
3. Huang, Y., von Eckardstein, A., Wu, S., and Assmann, G. (1995) Cholesterol efflux, cholesterol esterification, and cholesteryl ester transfer to LpA-I and LpA-I/A-II in native plasma, *Arterioscler., Thromb., Vasc. Biol. 15*, 1412−1418.
4. Lund-Katz, S., Hammerschlag, B., and Phillips, M. C. (1982) Kinetics and mechanism of free cholesterol exchange between human serum high- and low- density lipoproteins, *Biochemistry 21*, 2964−2969.
5. Miida, T., Fielding, C. J., and Fielding, P. E. (1990) Mechanism of transfer of LDL-derived free cholesterol to HDL subfractions in human plasma, *Biochemistry 29*, 10469−10474.
6. Sviridov, D., Miyazaki, O., Theodore, K., Hoang, A., Fukamachi, I., and Nestel, P. (2002) Delineation of the role of pre-β-1-HDL in cholesterol efflux using isolated pre-β- 1-HDL, *Arterioscler., Thromb., Vasc. Biol. 22*, 1482−1488.
7. Lee, M., Sommerhoff, C. P., von Eckardstein, A., Zettl, F., Fritz, H., and Kovanen, P. T. (2002) Mast cell tryptase degrades HDL and blocks its function as an acceptor of cellular cholesterol, *Arterioscler., Thromb., Vasc. Biol. 22*, 2086−2091.
8. Fielding, P. E., Kawano, M., Catapano, A. L., Zoppo, A., Marcovina, S., and Fielding, C. J. (1994) Unique epitope of apolipoprotein A−I expressed in pre-β-1 high-density lipoprotein and its role in the catalyzed efflux of cellular cholesterol, *Biochemistry 33*, 6981−6985.

9. Nanjee, M. N., Cooke, C. J., Garvin, R., Semeria, F., Lewis, G., Olszewski, W. L, and Miller, N. E. (2001) Intraveous apo A-1/ lecithin discs increase pre-beta HDL concentrations in tissue fluid and stimulate reverse cholesterol transport in humans, *J. Lipid Res*. *42*, 1586−1593.
10. Francone, O. L., Royer, L., and Haghpassand, M. (1996) Increased prebeta-HDL levels, cholesterol efflux, and LCAT-mediated esterification in mice expressing the human cholesteryl ester transfer protein (CETP) and human apolipoprotein A-1 (apo A-1) transgenes, *J. Lipid Res. 37*, 1268−1277.
11. Fielding, C. J., and Fielding, P. E. (1995) Molecular physiology of reverse cholesterol transport, *J. Lipid Res*. *36*, 211−228.
12. Duverger, N., Rader, D., Duchateau, P., Fruchart, J. C., Castro, G., and Brewer, H. B. (1993) Biochemical characterization of the three major subclasses of lipoprotein A-1 preparatively isolated from human plasma, *Biochemistry 32*, 12372−12379.
13. Barter, P. J., Brewer, H. B., Chapman, M. J., Hennekens, C. H., Rader, D. J., and Tall, A. R. (2003) Cholesteryl ester transfer protein: a novel target for raising HDL and inhibiting atherosclerosis, *Arterioscler. Thromb. Vasc. Dis. 23*, 160−167.
14. Krieger. M. (2001) Scavenger receptor class B type I is a multiligand HDL receptor that influences diverse physiologic systems, *J. Clin. Invest. 108*, 793−797.
15. Liang, H. Q., Rye, K. A., and Barter, P. J. (1995) Cycling of apolipoprotein A-I between lipid-associated and lipid-free pools, *Biochim. Biophys. Acta 1257*, 31−37.
16. Jiang, X., Francone., O. L., Bruce, C., Milne, R., Mar, J., Walsh, A., Breslow, J. L., and Tall, A. R. (1996) Increased prebeta− high-density lipoprotein, apolipoprotein AI, and phospholipid in mice expressing the human phospholipid transfer protein and human apolipoprotein AI transgenes, *J. Clin. Invest. 98*, 2373−2380.
17. Lie, J., de Crom, R., Jauhiainen, M., van Gent, T., van Haperen, R., Scheek, L., Jansen, H., Ehnholm, C., and van Tol, A. (2001) Evaluation of phospholipid transfer protein and cholesteryl ester transfer protein as contributors to the generation of prebeta high-density lipoproteins, *Biochem. J. 360*, 379−385.
18. Rye, K. A., Duong, M., Psaltis, M. K., Curtiss, L. K., Bonnet, D. J., Stocker, R., and Barter, P. J. (2002) Evidence that phospholipids play a key role in pre-β apo A-1 formation and high-density lipoprotein remodeling, *Biochemistry 41*, 12538−12545.
19. Miyazaki, O., Kobayashi, J., Fukamachi, I., Miida, T., Bujo, H., and Saito, Y. (2000) A new sandwich enzyme immunoassay for measurement of plasma prebeta1-HDL levels, *J. Lipid Res. 41*, 2083−2088.
20. Miida, T., Miyazaki, O., Nakamura, Y., Hirayama, S., Hanyu, O., Fukamachi, I., and Okada, M. (2003) Analytical performance of a sandwich enzyme immunoassay for prebeta1-HDL in stabilized plasma, *J. Lipid Res. 44*, 645−650.
21. Sviridov, D., Kingwell, B., Hoang, A., Dart, A., and Nestel, P. (2003) Single session exercise stimulates formation of prebeta1-HDL in leg muscle, *J. Lipid Res. 44*, 522−526.
22. Jafari, M., Leaf, D. A., Macrae, H., Kasem, J., O'Conner, P., Pullinger, C., Malloy, M., and Kane, J. P. (2003) The effects of physical exercise on plasma prebeta-1 high-density lipoprotein, *Metabolism 52*, 437−442.
23. Miida, T., Miyazaki, O., Hanyu, O., Nakamura, Y., Hirayama, S., Narita, I., Gejyo, F., Ei, I., Tasaki, K., Kohda, Y., Ohta, T., Yata, S., Fukamachi, I., and Okada, M. (2003) LCAT-dependent conversion of prebeta1-HDL into alpha-migrating HDL is severely delayed in hemodialysis patients, *J. Am. Soc. Nephrol. 14*, 732−738.
24. Brewer, H. B., Ronan, R., Meng, M., and Bishop, C. (1986) Isolation and characterization of apolipoproteins A-I, A-II and A-IV, *Methods Enzymol*. *128*, 223−246.
25. Reinhard, E. J., Wang, J. L., Durley, R. C., Fobian, Y. M., Grapperhaus, M. L., Hickory, B. S., Massa, M. A., Norton, M. B., Promo, M. A., Tollefson, M. B., Vernier, W. F., Connolly, D. T., Witherbee, B. J., Melton, M. A., Regina, K. J., Smith, M. E., and Sikorski, J. A. (2003) Discovery of a simple picomole inhibitor of cholesteryl ester transfer protein, *J. Med. Chem. 46*, 2152−2168.
26. Miida, T., Kawano, M., Fielding, C. J., and Fielding, P. E. (1992) Regulation of the concentration of pre-β high-density lipoprotein in normal plasma by cell membranes and lecithin: cholesterol acyltransferase activity, *Biochemistry 31*, 11112−11117.
27. Fielding, P. E., and Fielding, C. J. (1996) Intracellular transport of low-density lipoprotein derived free cholesterol begins at clathrin coated pits and terminates at cell surface caveolae, *Biochemistry 35*, 14932−14938.
28. Swaney, J. B., and O'Brien, K. (1978) Cross-linking studies of the self-association properties of apo A-1 and apo A-II from human high-density lipoprotein, *J. Biol. Chem. 253*, 7069−7077.
29. Fielding, C. J. (1985) Lecithin-cholesterol acyltransferase and cholesterol transport, *Methods Enzymol. 111*, 267−274.
30. Ogawa, Y., and Fielding, C. J. (1985) Assay of cholesteryl ester transfer activity and purification of a cholesteryl ester transfer protein, *Methods Enzymol. 111*, 274−285.
31. Jonas, A. (1998) Regulation of lecithin:cholesterol acyltransferase activity, *Prog. Lipid Res. 37*, 209−234.
32. Francone, O. L., and Fielding, C. J. (1991) Effects of site-directed mutagenesis at residues cysteine-31 and cysteine-184 on lecithin: cholesterol acyltransferase activity, *Proc. Natl. Acad. Sci. U.S.A. 88*, 1716−1720.
33. Qu, S. J., Fan, H. Z., Blanco-Vaca, F., and Pownall, H. J. (1993) Roles of cysteines in human lecithin:cholesterol acyltransferase, *Biochemistry 32*, 3089−3094.
34. Francone, O. L., and Fielding, C. J. (1991) Structure−function relationships in human lecithin:cholesterol acyltransferase. Site-directed mutagenesis at serine residues 181 and 216, *Biochemistry 30*, 10074−10077.
35. Citron, M., Diehl, T. S., Capell, A., Haass, C., Teplow, D. B., and Selkoe, D. J. (1996) Inhibition of amyloid beta-protein production in neural cells by the serine protease inhibitor AEBSF, *Neuron 17*, 171−179.
36. Huuskonen, J., Wohlfahrt, G., Jauhiainen, M., Ehnholm, C., Teleman, O., and Olkkonen, V. M. (1999) Structure and phospholipid transfer activity of human PLTP: analysis by molecular modeling and site-directed mutagenesis, *J. Lipid Res. 40*, 1123−1130.
37. Ponsin, G., Qu, S. J., Fan, H. Z., and Pownall, H. J. (2003) Structural and functional determinants of human plasma phospholipid transfer protein activity as revealed by site-directed mutagenesis of charged amino acids, *Biochemistry 42*, 4444−4451.
38. Schindler, P. A., Settineri, C. A., Collet, X., Fielding, C. J., and Burlingame, A. L. (1995) Site-specific detection and structural characterization of the glycosylation of human plasma proteins lecithin: cholesterol acyltransferase and apolipoprotein D using HPLC/electrospray mass spectrometry and sequential glycosidase digestion, *Protein Sci. 4*, 791−803.
39. Cheung, M. C., Wolf, A. C., Lum, K. D., Tollefson, J. H., and Albers, J. J. (1986) Distribution and localization of lecithin: cholesterol acyltransferase and cholesteryl ester transfer activity in A-1 containing lipoproteins, *J. Lipid Res. 27*, 1135−1144.
40. Kobori, K., Saito, K., Ito, S., Kotani, K., Manabe, M., and Kanno, T. (2002) A new enzyme-linked immunoabsorbent assay with two monoclonal antibodies to specific epitopes measures human lecithin: cholesterol acyltransferase, *J. Lipid Res. 43*, 325−334.
41. Chao, W. T., Fan, S. S., Chen, J. K., and Yang, V. C. (2003) Visualizing caveolin-1 and HDL in cholesterol-loaded aortic endothelial cells, *J. Lipid Res. 44*, 1094−1099.
42. Favari, E., Lee, M., Calabresi, L., Franceschini, G., Zimetti, F., Bernini, F., and Kovanen, P. T. (2004) Depletion of pre-beta-high-density lipoprotein by human chymase impairs ATP-binding cassette transporter A1- but not scavenger receptor class BI-mediated lipid efflux to high-density lipoprotein, *J. Biol. Chem. 279*, 9930−9936.
43. Kunitake, S. T., Chen, G. C., Kung, S. F., Schilling, J. W., Hardman, D. A., and Kane, J. P. (1990) Prebeta high-density lipoprotein. Unique disposition of apolipoprotein A-1 increases susceptibility to proteolysis, *Arteriosclerosis 10*, 25−30.
44. von Eckardstein, A., Jauhiainen, M., Huang, Y., Metso, J., Langer, C., Pussinen, P., Wu, S., Ehnholm, C., and Assmann, G. (1996) Phospholipid transfer protein mediated conversion of high-density lipoproteins generates prebeta-1 HDL, *Biochim. Biophys. Acta 1301*, 255−262.
45. Dullaart, R. P., and van Tol, A. (2001) Role of phospholipid transfer protein and prebeta-high-density lipoproteins in maintaining cholesterol efflux from Fu5AH cells to plasma from insulin-resistant subjects, *Scand. J. Clin. Lab. Invest. 61*, 69−74.
46. Asztalos, B. F., Sloop, C. H., Wong, L., and Roheim, P. S. (1993) Two-dimensional electrophoresis of plasma lipoproteins: recognition of new apo A-1-containing subpopulations, *Biochim. Biophys. Acta 1169*, 291−300.
47. Brites, F. D., Cavallero, E., de Geitere, C., Nicolaiew, N., Jacotot, B., Rosseneu, M., Fruchart, J. C., Wikinski, R. L., and Castro, G.

R. (1999) Abnormal capacity to induce cholesterol efflux and a new Lp-AI prebeta-particle in type 2 diabetic patients, *Clin. Chim. Acta 279*, 1−14.

48. Sparks D. L., Frank, P. G., Braschi, S., and Neville, T. A., and Marcel, Y. L. (1999) Effect of apolipoprotein A-1 lipidation on the formation and function of pre-β- and α-migrating LpA-1 particles, *Biochemistry 38*, 1727−1735.
49. Denis, M., Haidar, B., Marcil, M., Bouvier, M., Krimbou, L., and Genest, J. (2004) Molecular and cellular physiology of apolipoprotein A−I lipidation by the ATP-binding cassette transporter A1 (ABCA1), *J. Biol. Chem. 279*, 7384−7394.
50. Thuahnai, S. T., Lund-Katz S., Williams D. L., and Phillips M. C. (2001) Scavenger receptor class B, type I-mediated uptake of various lipids into cells. Influence of the nature of the donor particle interaction with the receptor, *J. Biol. Chem. 276*, 43801−43808.
51. Liadaki, K. N., Liu T., Xu S., Ishida, B. Y., Duchateaux, P. N., Krieger, J. P., Kane, J., Krieger, M., and Zannis, V. I. (2000) Binding of high-density lipoprotein (HDL) and discoidal reconstituted HDL to the HDL receptor scavenger receptor class B type I. Effect of lipid association and APOA-I mutations on receptor binding, *J. Biol. Chem. 275*, 21262−21271.
52. Fielding, C. J., Bist, A., and Fielding P. E. (1999) Intracellular cholesterol transport in synchronized human skin fibroblasts, *Biochemistry 38*, 2506−2513.
53. Hui, D. Y., and Howles, P. N. (2002) Carboxyl ester lipase: structure−function relationship and physiological role in lipoprotein metabolism and atherosclerosis, *J. Lipid Res. 43*, 2017−2030.

BI0485629